J. Membrane Biol. 172, 193–201 (1999)

The Journal of
Membrane
Biology

A 59 Amino Acid Insertion Increases Ca^{2+} Sensitivity of *rbslo1*, a Ca^{2+}-Activated K^+ Channel in Renal Epithelia

K. Hanaoka, J.M. Wright, I.B. Cheglakov, T. Morita, W.B. Guggino
The Johns Hopkins University School of Medicine, Department of Physiology, Baltimore, MD 21205, USA

Received: 23 August 1999

Abstract. We previously cloned a MaxiK channel α-subunit isoform, *rbslo1,* from rabbit kidney with an amino acid sequence highly homologous to *mslo* but with a 59 amino acid insertion between S8 and S9 (Morita et al., 1997. *Am. J. Physiol.* **273:**F615–F624). *rbslo1* activation properties differed substantially from *mslo* with much greater Ca^{2+} sensitivity, half-activation potential of −49 mV in 1 μM Ca^{2+}. We now report single-channel analysis of *rbslo1* and *delA,* a construct produced by removal of the 59 amino acid insertion at site A. *delA* is identical to *mslo* from upstream of S1 to downstream of S10 with the exception of 8 amino acids. Slope of the steady-state Boltzmann voltage activation curve was 8.1 mV per e-fold change in probability of opening for both *rbslo1* and *delA.* The apparent $[Ca^{2+}]_i$ properties in *delA* were more like *mslo* but the voltage-activation properties remained distinctly *rbslo1*. Ca^{2+} affinity decreased and transmembrane voltage effects on apparent Ca^{2+} affinity increased in *delA.* The differences between *rbslo1* and other cloned channels appear to be localized at insertion site A with both the insertion sequence and amino acid substitutions near site A being important. The steeper activation slope makes the channel more responsive to small changes in transmembrane voltage while the insertion sequence makes the channel functional at physiological low levels of $[Ca^{2+}]_i$.

Key words: Potassium channel — BK channel — Gating — Single-channel recording

Introduction

Large conductance (maxi), Ca^{2+}-activated K^+ channels are expressed in several nephron segments (Guggino et al., 1987; Merot et al., 1989; Ling, Hinton & Eaton, 1991; Morita et al., 1997). However, the role of Ca^{2+}-activated K^+ channels in renal function is still unresolved. We have shown in cultured kidney cells that forskolin and ADH can activate Ca^{2+}-activated K^+ channels probably via phosphorylation of the channel protein (Guggino et al., 1985). This suggests that under some stimulated conditions Ca^{2+}-activated K^+ channels may indeed play a role in transcellular transport. Two subunits of maxi K^+ channels have been cloned (Butler et al., 1993; Knaus et al., 1994). The α subunit is the functional unit that is inhibited by iberiotoxin (IBTX). The β subunit does not produce any current when it is expressed in *Xenopus* oocytes. However, co-expression of the α and β subunits in *Xenopus* oocytes produces currents with increased Ca^{2+}- and voltage-sensitivity, compared with the current produced by expression of α subunit alone (*see* McManus et al. (1995) for a discussion). Although maxi K^+ channels are known to exist in several nephron segments, the distribution and the abundance of these channels at protein level in each cell type has not been reported nor has the cellular localization been established.

We previously cloned and reported a MaxiK channel α-subunit isoform, *rbslo1,* from rabbit medullary thick ascending limb cell line (mTAL cell) (Morita et al., 1997). The amino acid sequence of *rbslo1* is highly homologous to MaxiK channels cloned from other species such as *mslo, hslo,* and *cslo.* Sequences between *rbslo1* and *hslo1* are very similar except for an additional 44 amino acid group at the C-terminal and alternative splicing site A (Morita et al., 1997). At site A (*see* Fig. 1*A*), *rbslo1* has a sequence of 59 amino acids which differs by 8 amino acids from an insertion found at the same site in rat PC-12 cells (Fig. 1*B*) (Saito et al., 1997).

We have used two expression systems (*Xenopus* oocytes and CHO cells) to characterize the channels. The unique feature of *rbslo1* is greatly enhanced Ca^{2+}- and

Correspondence to: W.B. Guggino

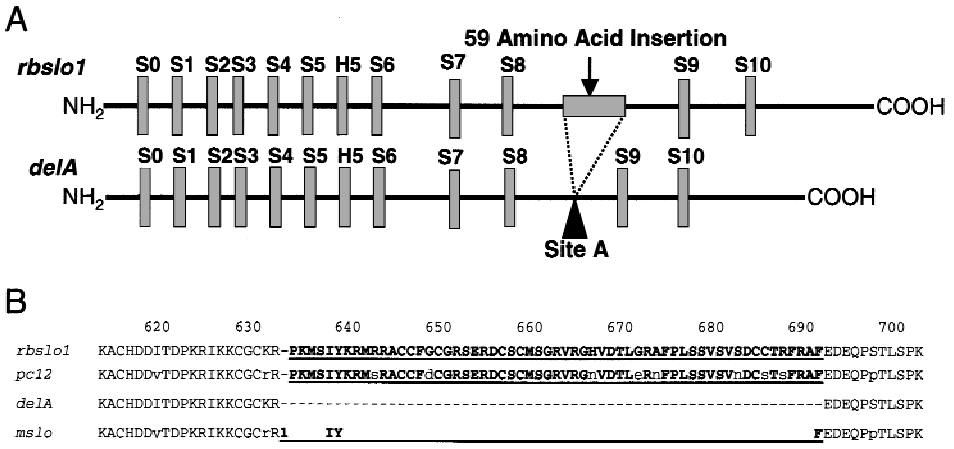

Fig. 1. (*A*) Schematic drawing of the MaxiK channel α-subunit from rabbit kidney (*rbslo1*) and the deletion mutation (*delA*) used in these experiments. The hydrophobic segments (S0–S10) and pore-forming loop (H5) are indicated with filled boxed. The 59 amino acid sequence shown in *rbslo1* was deleted to produce *delA*. The location of alternative splicing site A (▲) is indicated in *delA*. Hydrophobic regions drawn and numbered after Wallner, Meera & Toro (1996) and Meera et al. (1997). (*B*) Insertion sequence data (underlined) comparing *rbslo1* with *rslo* from PC-12 cells and *delA* with *mslo.*

voltage sensitivities compared to previously cloned α subunits. For example, the membrane potential to achieve a half-maximal conductance ($V_{1/2}$) for *rbslo1* expressed in CHO cells is 61 mV at 0.1 μM Ca^{2+} and −33 mV at 1 μM Ca^{2+} in symmetrical 150 mM $[K^+]$. In comparison, for the *hslo* channel (hbr5), $V_{1/2}$ at 2.4 μM $[Ca^{2+}]_i$ with symmetrical 110 mM $[K^+]$ is about 0 mV (Tseng-Crank et al., 1994) much more positive than what we observed for the *rbslo1* channel (*see* Morita et al., 1997). This raised the intriguing possibility that splice variants of Ca^{2+}-activated K^+ channels with enhanced Ca^{2+}-sensitivity do play a role in distal tubule K^+ transport under normal circumstances and in disease states.

Because other studies indicated that alternative splicing at site A modified channel sensitivity to $[Ca^{2+}]_i$ (Lagrutta et al., 1994; Saito et al., 1997; Xie & McCobb, 1998), we hypothesized that the insertion sequence at site A altered the Ca^{2+} sensitivity of *rbslo1*. Therefore we created a mutation, *delA*, where the 59 amino acids from site A were removed (Fig. 1). Our results indicated that deletion of the 59 amino acid sequence at site A resulted in functional changes in the sensitivity to $[Ca^{2+}]_i$.

Materials and Methods

Expression in CHO Cells

rbslo1 cloned from cDNA library of rabbit medullary thick ascending limb cell line (mTAL cells) was expressed in mammalian cells using pGFP-N1 vector (Clontech, Palo Alto, CA) (Morita et al., 1997). In brief, XbaI restriction site was created in place of NdeI restriction site after stop codon of *rbslo1*. SalI and XbaI were used to cut out the fragment of cDNA coding for GFP protein, then cDNA coding for *rbslo1* was introduced into the vector. Deletion mutant, *delA,* was made by a protocol previously described (Devidas, Yue & Guggino, 1998). *rbslo1* and *delA* plasmid DNAs were prepared by cesium trifluoroacetate centrifugation method.

Chinese hamster ovary–K1 cells (CHO cells) were obtained from American Type Culture Collection (Rockville, MD) and grown in a culture flask containing: 90% Ham's F-12 medium (Mediatech, Herndon, VA) and 10% fetal bovine serum (Hyclone, Logan, UT). Cells were replated on glass coverslips (Belleco Glass, Vineland, NJ) 24 hr before transfection. Calcium phosphate precipitation method was employed to transfect plasmids into CHO cells. An expression construct containing the murine T-lymphocyte-specific surface protein CD4, was cotransfected (Morita et al., 1997) and cells expressing CD4 were identified by attachment of CD4 antibody-coated beads (Dynail, Lake Success, NY). Ca^{2+}- and voltage-activated K^+ currents were found in 95% of cells with attached CD4 antibody-coated beads. *rbslo1* or *delA* currents were recorded in 24–72 hr after transfection only from cells with attached beads.

Electrophysiology

Single-channel recordings from inside-out patches were performed as described by Hamill et al. (1981) using an EPC-7 patch-clamp amplifier (List Electronic, Darmstadt, Germany) with pClamp version 6.0.2 software (Axon Instruments, Foster City, CA). Patch pipettes were pulled from borosilicate glass (15–20 MΩ; WPI, Sarasota, FL), coated with Sylgard® and fire-polished. Recordings were initially filtered at 10 kHz through the low-pass Bessel filter in the EPC–7 amplifier, digitized and recorded on videotape (VR-10B, Instrutech, Great Neck, NY). Data were replayed and refiltered through an 8-pole low-pass Bessel filter at 1 kHz (Model 902, Frequency Devices, Haverhill, MA), digitized at 5 kHz (ISC-16, RC Electronics, Goleta, CA) for analysis.

The pipette (extracellular) solution contained (in mM): 150 KCl, 1 $MgCl_2$, 10 HEPES, and 1 EGTA (pH 7.4); 118 μM $CaCl_2$ was added to bring the free Ca^{2+} to 10^{-8} M as calculated by the program Bound and Determined (Brooks & Storey, 1992). The bath solution contained (in mM): 150 KCl, 1 $MgCl_2$, 10 HEPES, and 1 EGTA (pH 7.4). The free Ca^{2+} concentration was adjusted by adding $CaCl_2$. A Ca^{2+}-selective electrode sensitive to 0.1 μM free Ca^{2+} (Okada, Hazama & Oiki, 1988)

was manufactured and calibrated against reference solutions (WPI, Sarasota, FL) to check free Ca^{2+} concentration of the solutions. A multibarrel perfusion system was used to quickly change bath solutions. Experiments were performed at room temperature (23–26°C).

Data Analysis

Data analysis was done using software previously described (Wright, Kline & Nowak, 1991). In brief, threshold of channel opening was set at 50% of the unit single-channel current. Mean open time was obtained from an open-time histogram constructed from an event list. Burst analysis was done only on recordings that had a clear separation between short and long closed time; bursts were defined as described by Colquhoun and Sakmann (1985). Open-, closed- and burst-time data were fitted by maximum likelihood method before binning as described by Colquhoun and Sigworth (1995). Most experiments were performed on patches containing a single MaxiK channel. Patches containing 2 or 3 channels were used only for open probability (P_o) and mean open-time analysis. ALLFIT (DeLean, Munson & Rodbard, 1978) was used for evaluating concentration-response curves by simultaneous fitting of the data set. The Excel statistical package was used for *t*-tests. Boltzmann function model fitting was done in Origin (MicroCal, Andover, MA). Data are reported as mean ± SEM; differences are regarded as significant for $P < 0.05$.

Results

Single-Channel Properties of *rbslo1* and *delA*

This is the first detailed report on the activation properties of *rbslo1* and *delA* produced by analysis of single-channel properties of the channels. Figure 2 shows representative recordings of *rbslo1* and *delA* in 1 μM of $[Ca^{2+}]_i$, at different holding voltages. In 0.3 to 1 μM $[Ca^{2+}]_i$ the single-channel conductance of *rbslo1* (245.3 ± 4.2 pS, $n = 6$) was not significantly different from *delA* (248.3 ± 5.6 pS, $n = 7$; Fig. 2*B*).

Changes in mean open time, burst duration and number of events per burst at different membrane potentials are shown in Fig. 3. All of the data were recorded at 1 μM $[Ca^{2+}]_i$. Typical of Ca^{2+}-activated K^+ channels, the mean open time, burst duration and number of events per burst of *rbslo1* (filled circles) increases as transmembrane voltage becomes more positive (Fig. 3*A–C*). This is consistent with previous data that Ca^{2+}-activated K^+ channels have a sensor that detects transmembrane voltage (Cui, Cox & Aldrich, 1997). Similar to *rbslo1*, the mean open time, burst duration and number of events per burst for *delA* (open circles) also increases as transmembrane voltage becomes more positive (Fig. 3*A–C*). In contrast, however, the *delA* (open circles) channel had an almost parallel shift to the right in all of the parameters measured (Fig. 3*A–C*). Compared to *rbslo*, *delA*, requires more positive voltages for activation to occur.

To determine how the *delA* construct affects channel gating kinetics, we plotted the mean open time, burst duration and number of events per burst against the P_o among patches at the same holding potential (Fig. 3*D–F*). The data show that at equivalent values of P_o for *rbslo1* and *delA* there is no difference between the channels in mean open time, burst duration and number of events per burst. Thus, although it takes more positive voltages for *delA* to achieve the same open probability as *rbslo1*, once *delA* achieves the same open probability, as *rbslo1* there is no difference in channel behavior.

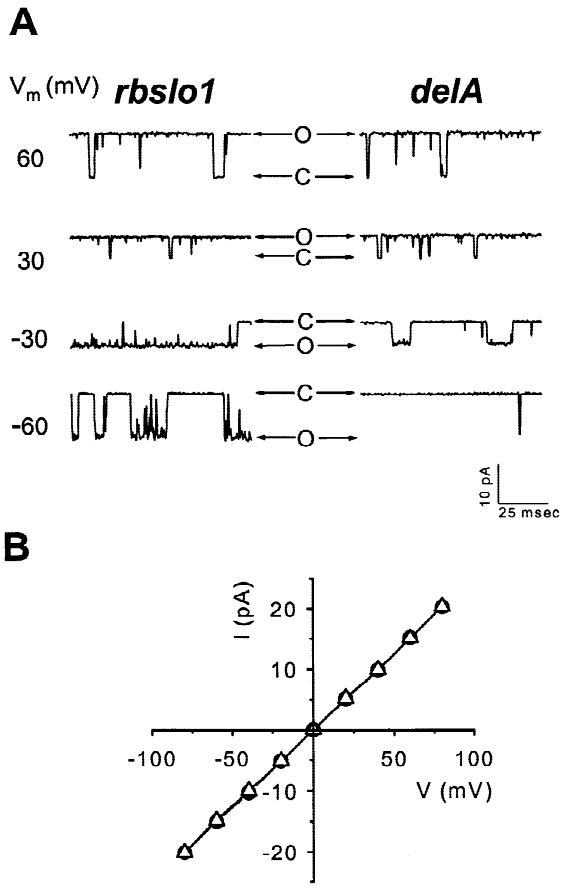

Fig. 2. Single-channel conductance *I–V* plot. (*A*) Single channel currents from *rbslo1* and *delA* recorded in the presence of 1 μM $[Ca^{2+}]_i$ at −60, −30, +30 and +60 mV membrane potential. Channel open and closed states are indicated as O and C, respectively. (*B*) Single-channel conductances were 245.3 ± 4.2 pS ($n = 6$) for *rbslo1* and 248.3 ± 5.6 pS ($n = 7$) for *delA*. Filled and open circles indicate mean current amplitude at each membrane potential for *rbslo1* and *delA* respectively. Bars indicate SEM.

Looking at the individual parameters more closely, it is evident that burst duration of *rbslo1* and *delA* increased fourfold from 5.7 msec to 23.2 msec as P_o changed eightfold from 0.1 to 0.8 (Fig. 3*E*). An increase in mean open time as well as number of openings per burst contributed to extend burst duration at depolarized membrane potentials.

Closed times were fit with two exponential components in a wide range of P_o (*data not shown*). The closed

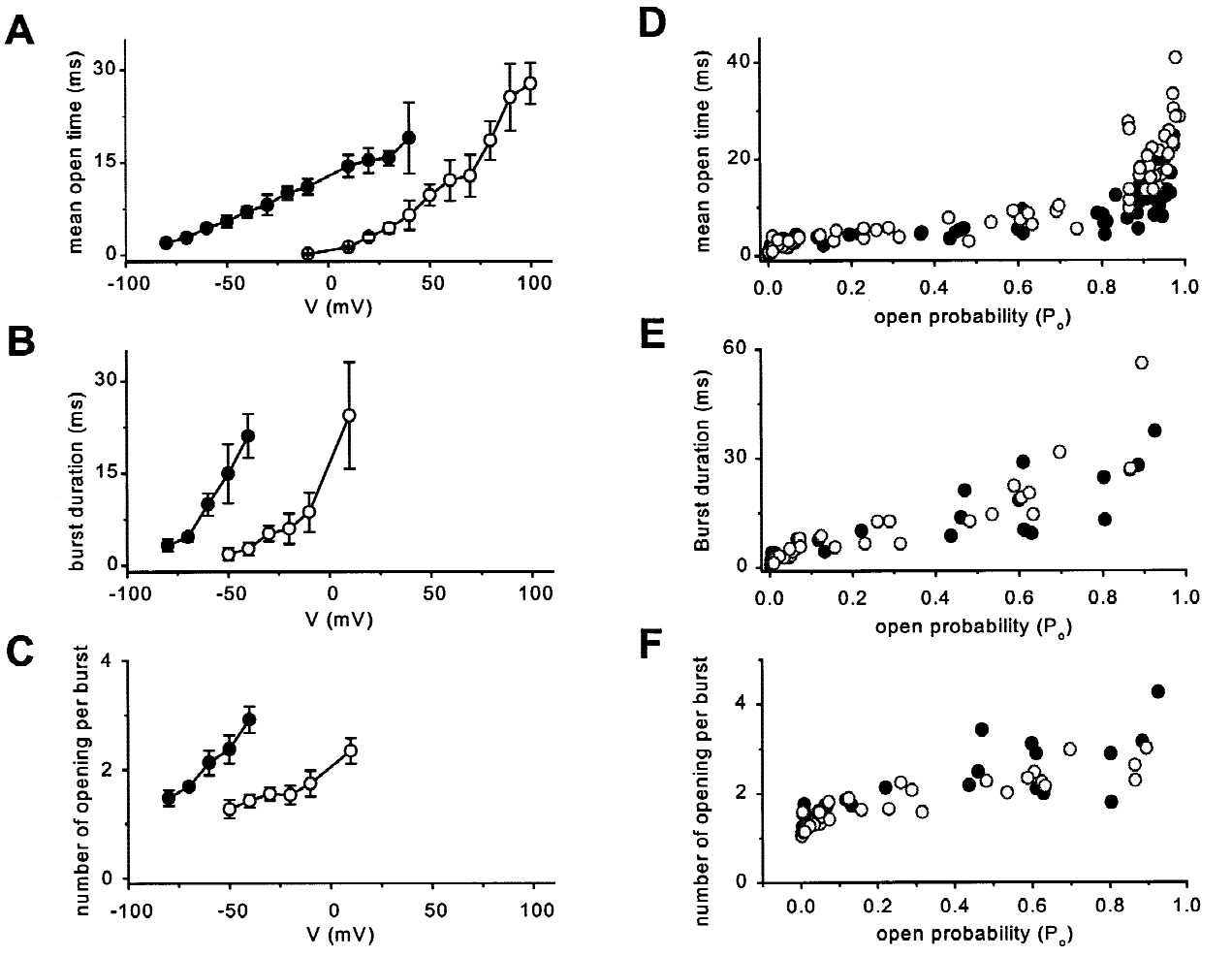

Fig. 3. Single-channel gating properties plotted as a function of voltage (*A, B, C*) and P_o (*D, E, F*). Variability of P_o in individual patches contributed to variability of measurements for mean open time (*A*), burst duration (*B*), and number of events per burst (*C*). Despite differences in activation threshold voltages, mean open time (*D*), burst duration (*E*) and number of openings per burst (*F*) were unaffected in *delA* when plotted as a function of P_o. Data were recorded in the presence of 1 μM Ca^{2+}. Filled circles are *rbslo1* and open circles are *delA*. Each point represents the mean of at least 3 patches and bars indicate SEM in *A, B, C.* Individual data points shown in *D, E, F.*

time of the interburst interval decreased as P_o increased. Within the burst, closed times did not significantly change with voltage or P_o (0.46 ± 0.06 msec at −80 mV, $n = 3$; 0.39 ± 0.05 msec at −60 mV, $n = 3$; and 0.42 ± 0.03 msec at −40 mV, $n = 5$ for *rbslo1*). And, there was no significant difference in short closed times between *rbslo1* and *delA* (0.44 ± 0.03 msec, $n = 21$ *vs.* 0.46 ± 0.05 msec, $n = 35$). Analysis of closed times was consistent with the finding that changes in interburst interval a major factor in the changes P_o induced by changes in transmembrane voltage.

Voltage-Dependent Activation of *rbslo1* and *delA*

The voltage-dependent behavior of open probability (P_o) was modeled with the Boltzmann function:

$$P_o = 1/[1 + \exp^{-(V-V_{1/2})zF/RT}], \quad (1)$$

where $V_{1/2}$ is the membrane potential at which half of channel activation is observed; *F, V, R* and *T* have their usual thermodynamic meanings. The amount of charge moving between opposite sides of the membrane is the gating charge, *z*, and governs the change in P_o with voltage.

Steady-state voltage-activation curves were well fit by a single Boltzmann at all tested $[Ca^{2+}]_i$ (Fig. 4). Gating charge was not significantly different between *rbslo1* (2.91 ± 0.41; $n = 6$) and *delA* (2.98 ± 0.2 $n = 7$) in 1 μM $[Ca^{2+}]_i$. From *z*, we calculated the e-fold change of P_o against membrane potential for *rbslo1* as 8.1 ± 0.8 mV ($n = 6$) and 8.9 ± 1.1 mV ($n = 7$) for *delA*. Hence, there was no indication that insertion of 59 amino acids

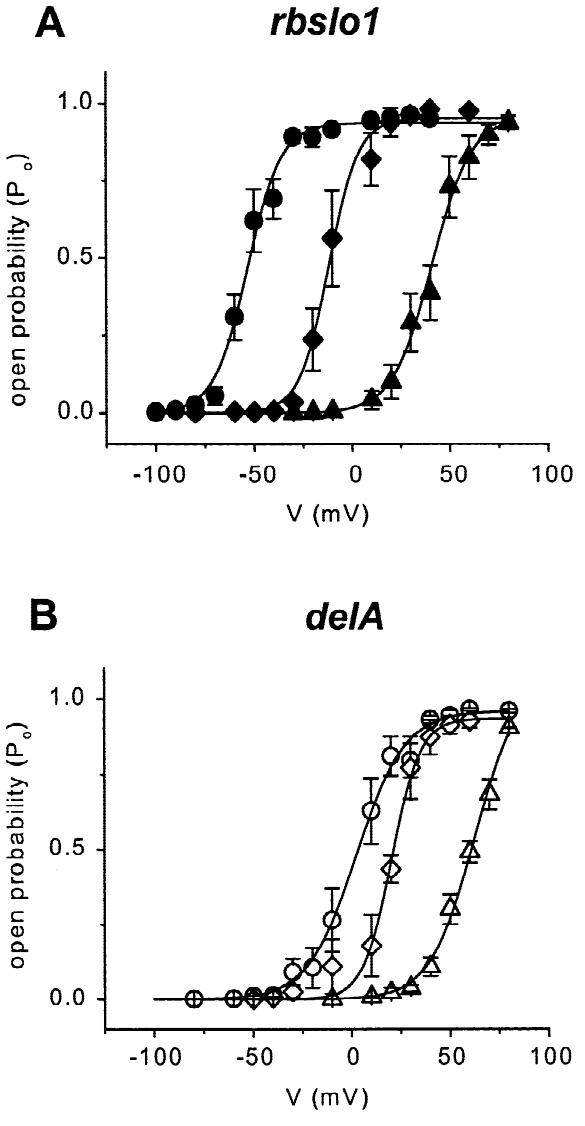

Fig. 4. Boltzmann fitting of steady-state voltage-dependent channel activation data. *rbslo1* (*A*) activated at more negative potentials than *delA* (*B*). Tested $[Ca^{2+}]_i$ were 1 μM (circle), 0.65 μM (diamond) and 0.3 μM (upper triangle). Continuous curves are best fits of Boltzmann functions. Each data point was the average of at least 3 experiments; bars indicate SEM.

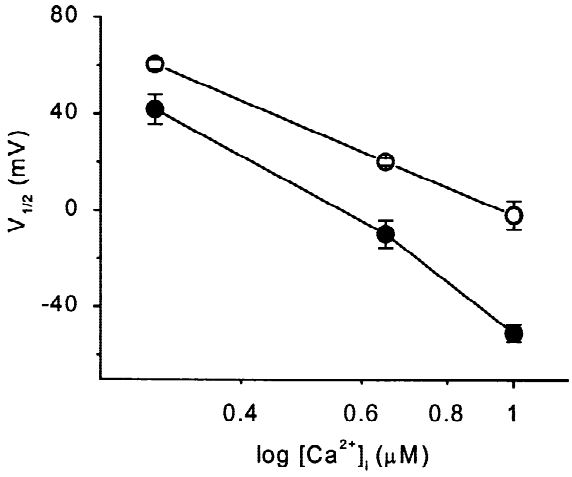

Fig. 5. $V_{1/2}$ *vs.* $[Ca^{2+}]_i$. The shift in the membrane potential at which half-maximal channel activation occurred was not parallel. Filled circles are *rbslo1,* open circles are *delA.* Bars indicate SEM. Data are from Boltzmann fittings shown in Fig. 4.

at site A of *rbslo1* had direct influence on the response of the voltage sensor to changes in voltage.

Effects Ca^{2+} Activation

Although the slopes of the activation curves were unchanged, there were two substantial differences in $V_{1/2}$ between *rbslo1* and *delA*. First, *rbslo1* was much more sensitive to $[Ca^{2+}]_i$ than *delA* with a $V_{1/2}$ in 0.3 μM of 39.7 ± 4.3 mV for *rbslo1* and 60.6 ± 2.6 mV for *delA* (Figs. 4 and 5). Second, when the $V_{1/2}$ for the two clones was graphed against $[Ca^{2+}]_i$, it was apparent that the shift was not parallel over the ranges of $[Ca^{2+}]_i$ tested (Fig. 5). When $[Ca^{2+}]_i$ was increased from 0.3 to 1 μM, *rbslo1* $V_{1/2}$ shifted almost 90 mV to −49.3 ± 3.5 mV (Fig. 5). Yet, for the same $[Ca^{2+}]_i$ change, $V_{1/2}$ for *delA* changed less than 60 mV to 1.2 ± 6.1 mV (Fig. 5).

There were no indications of changes in the voltage sensor or single-channel properties, yet there were significant differences in $V_{1/2}$ at the same $[Ca^{2+}]_i$. Therefore, we next examined the effects of the deletion on apparent $[Ca^{2+}]_i$ affinity using the Hill equation:

$$P_o = 1/(1 + (K_d/[Ca^{2+}]_i)^n) \quad (2)$$

where n is the Hill coefficient, and K_d is the apparent Ca^{2+} dissociation constant.

The Hill coefficient (n_H) is often used to estimate the minimum number of bound Ca^{2+} required to fully activate the channels and is highly dependent upon the degree of cooperativity among binding sites in producing a measurable effect (McManus & Magleby, 1991; Cui et al., 1997). The relationship between $[Ca^{2+}]_i$ and P_o for *rbslo1* and *delA* is plotted in Fig. 6*A* and *B* respectively, where continuous lines indicate the fit with the Hill equation. The n_H for individually fitted *rbslo1* data sets ranged from 4.9 to 6.6 (Table). Immediately apparent is the difference between the n_H in each data set and the change in n_H with voltage in the *delA* protein. The family of concentration-response curves for *rbslo1* could be fit using an n_H of 5.7 ± 0.4 at all voltages without significantly degrading the goodness of fit ($P > 0.84$). There was considerable variability for *delA* (Table) and a substantial reduction in n_H at more negative holding potentials. The *delA* family of curves could not be fit with a single n_H ($P < 0.01$).

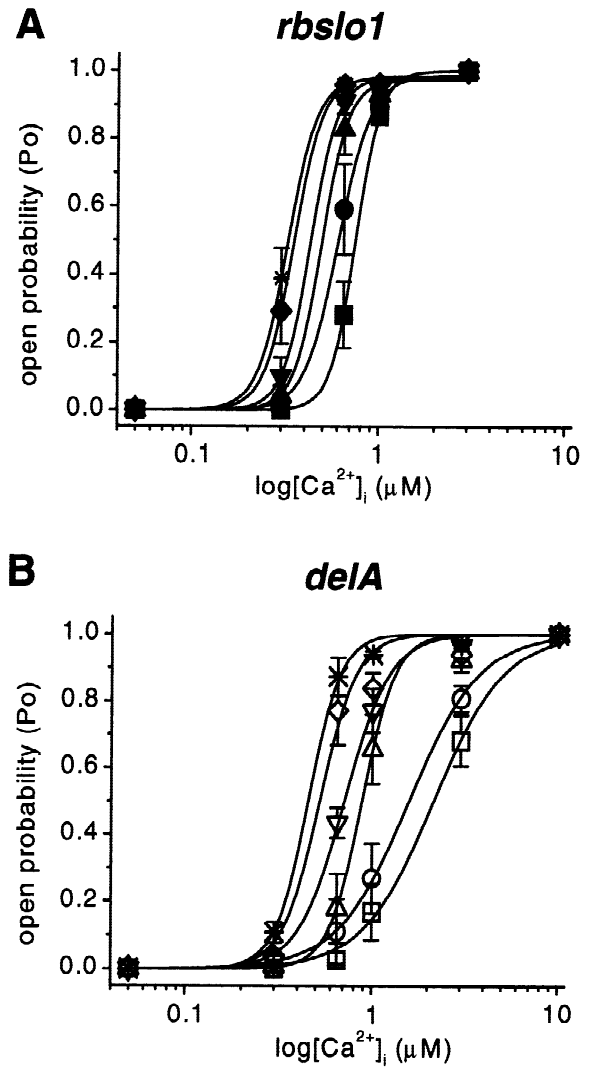

Fig. 6. Concentration-response curves of P_o *vs.* $[Ca^{2+}]_i$ for *rbslo1* and *delA*. The relationship P_o for *rbslo1* (*A*) and *delA* (*B*) *vs.* $[Ca^{2+}]_i$ was plotted for six different membrane potentials on semi-logarithmic coordinates. Results indicated a reduction in the apparent Ca^{2+} binding affinity for *delA*. Changes in slope do not account for the differences in K_d. Values are listed in the Table. The membrane potentials tested were: −20 mV (square), −10 mV (circle), 10 mV (up triangle), 20 mV (down triangle), 30 mV (diamond), and 40 mV (star). Continuous lines are Hill equation fits.

Table. Hill coefficient (n_H) and K_d

V_m†	*rbslo1*		*delA*	
	K_d (μM)	n_H	K_d (μM)	n_H
−20 mV	0.75 ± <0.01*	6.58 ± 0.02	2.14 ± 0.09	2.32 ± 0.17
−10 mV	0.60 ± 0.02	4.95 ± 0.8	1.58 ± 0.04	2.30 ± 0.08
10 mV	0.49 ± 0.02	6.07 ± 0.92	0.88 ± 0.03	4.94 ± 0.69
20 mV	0.43 ± 0.02	6.09 ± 0.06	0.71 ± <0.01	3.6 ± 0.27
30 mV	0.35 ± 0.01	5.71 ± 1.12	0.52 ± 0.04	4.45 ± 1.2
40 mV	0.32 ± 0.01	5.59 ± 2.04	0.45 ± 0.02	5.06 ± 0.44

* Values given as mean ± SEM.
† Transmembrane potential.

Discussion

rbslo1 has a 59 amino acid insertion created by alternate splicing at site A and has single-channel properties with two major functional differences when compared with other cloned MaxiK channels. *rbslo1* exhibits a much greater sensitivity to $[Ca^{2+}]_i$ and has a much steeper Boltzmann voltage activation curve than clones not having the insertion. Clones not having the insertion have been studied in a variety of expression systems and recording configurations. Despite the differences in experimental conditions, there is little variation in results. For example, the Ca^{2+} sensitivity and voltage-dependent activation of MaxiK channel clones have been studied in macropatches pulled from *Xenopus* oocytes expressing *mslo* (Cui et al., 1997); *hslo* (Tseng-Crank et al., 1994; McCobb et al., 1995), or *rslo* (Saito et al., 1997; Xie & McCobb, 1998). In the oocyte expression system, *mslo* results are consistent whether using single-channel (Butler et al., 1993) or macropatch (Cui et al., 1997) configurations. While it is possible our mammalian cell expression system is partially responsible for some of the altered dynamic characteristic of *rbslo1,* the voltage-activation characteristics of *hslo1.1* are the same whether expressed in CHO cells or oocytes (McCobb et al., 1995). Also, MaxiK channels in rat muscle behave much like *mslo,* with the native rat channel having a $[Ca^{2+}]_i$ affinity of 9 to 14 μM (McManus & Magleby, 1991).

Because of substantial difficulty in controlling and measuring $[Ca^{2+}]_i$ in an intact cell, only recently has there been an in depth study of Ca^{2+} sensitivity and n_H from on-cell patches of intact mammalian cells (Muñoz, Garcia & Guerrero-Hernandez, 1998). By combining fura-2 imaging, single-channel recording, and ionomycin-induced changes in $[Ca^{2+}]_i$, Muñoz et al. (1998) were able to document MaxiK channels with a 10-fold greater sensitivity than *mslo* to $[Ca^{2+}]_i$, and n_H with more than double the typical *mslo* values. In an excised patch, our cloned rabbit MaxiK channel with the insertion sequence, has $[Ca^{2+}]_i$ sensitivity and n_H values similar to those reported by Muñoz et al. (1998) for intact cell recordings. Removal of the insertion created a channel, *delA,* with properties more like those previously reported for MaxiK channels studied in excised patches.

The steepness of the Boltzmann activation curve is not related to the insertion because both *rbslo1* and *delA* have the same slope of 8.1 ± 0.8 mV per e-fold change in P_o. The closest value reported is from single-channel recordings of native MaxiK channels in cultured rat cells

with an e-fold change in P_o for 12 mV increment (Rothberg & Magleby, 1999). In expressed clones, the slope of the activation curve was 17 mV per e-fold change in *rslo* (Xie & McCobb, 1998) and ~15 mV per e-fold change for *mslo* (Butler et al., 1993; Cui et al., 1997). Although the *rbslo1* P_o sensitivity to voltage is about double the previously reported values of other clones and greater than values reported for native channels, this is well within the upper limit of ~4 mV per e-fold change estimated by Cui et al. (1997). The reduced steepness of the *mslo* voltage-activation curve compared with *rbslo1* would be consistent with *mslo* having fewer positive charges in the S4 segment (Hille, 1992). Yet, the *rbslo1* S4 region is identical with the *mslo* S4 region. Hence, differences in voltage-dependent gating must be due to changes outside the voltage sensor region and independent of the insertion. Given the very high homology of *rbslo1* and *mslo* (Morita et al., 1997), the critical differences are likely to lie in the 8 amino acid substitutions near site A.

The difference in $V_{1/2}$ between *rbslo1* and other clones was substantial and modulated by the insertion. At 1 μM $[Ca^{2+}]_i$, *rbslo1* $V_{1/2}$ was −49 mV, a difference of almost 130 mV from the *rslo* $V_{1/2}$ of +80 mV at the same concentration (Saito et al., 1997). Removal of the insertion lessened $[Ca^{2+}]_i$ sensitivity with *delA* having $V_{1/2}$ of −2 mV in 1 μM $[Ca^{2+}]_i$. Because of the large difference in sensitivity to $[Ca^{2+}]_i$, studies of other clones have usually been conducted at the higher $[Ca^{2+}]_i$ of 10 μM. Even in higher $[Ca^{2+}]_i$, their $V_{1/2}$ values did not approach the values for *rbslo1*. $V_{1/2}$ for *mslo* was reported as 23.4 mV (Butler et al., 1993) to 29.9 (Cui et al., 1997); $V_{1/2}$ for *rslo* was reported in the range of −2.3 (Xie & McCobb, 1998) to −10 (Saito et al., 1997); *hslo* $V_{1/2}$ was 12 mV (Wallner et al., 1996). A shift in $V_{1/2}$ has previously been reported for variety of insertions at site A. A 29 amino acid insertion in human atrial smooth muscle MaxiK channels results in a 10-fold higher sensitivity to $[Ca^{2+}]_i$ (McCobb et al., 1995). Saito et al. (1997) found that the 59 amino acid insertion at site A in *rslo* from PC-12 cells increased $[Ca^{2+}]_i$ sensitivity and shifted the activation curves 20 mV leftward. This insertion sequence from PC12 cells differs by only 8 amino acids from the *rbslo1* insertion (Fig. 1*B*) yet, produced a much less pronounced shift in $V_{1/2}$.

The MaxiK β-subunit is also capable of shifting $V_{1/2}$ 100 mV when co-expressed with *rslo* (Meera et al., 1997). *rbslo1* has the 41 amino acid sequence at the *N* terminus necessary for β-subunit regulation of Ca^{2+} activation. It is possible but very unlikely that the insertion interacts with the N-terminal modulatory site because there is no sequence homology between the β-subunit and the insertion sequence. In addition to the shift in $V_{1/2}$, *rbslo1* was extremely sensitive to changes in $[Ca^{2+}]_i$ with a shift of almost 90 mV for a 3-fold increase in $[Ca^{2+}]_i$ from 0.3 to 1 μM. In *delA*, the shift in $V_{1/2}$ was reduced to 60 mV for the same 3-fold change. In contrast *mslo* $V_{1/2}$ shifted only 42 mV for a 10-fold change in $[Ca^{2+}]_i$ (Butler et al., 1993). Although *delA* was more like *mslo* in that it was less sensitive to $[Ca^{2+}]_i$ manipulations than *rbslo1*, there were still substantial differences between it and *mslo*. Again indicating that small differences in the highly homologous proteins were important in regulation of $[Ca^{2+}]_i$ response.

MaxiK channel α-subunits form homotetrameric channels (Shen et al., 1994) and are modeled with four Ca^{2+} binding sites, one on each subunit (Cox, Cui & Aldrich, 1997). However, Schreiber and Salkoff (1997) have reported evidence for 2 Ca^{2+} binding domains in each subunit. The reported n_H in both native and cloned MaxiK channels have generally ranged from 2 to 3 (Barrett, Magleby & Pallotta, 1982; Cornejo, Guggino & Guggino, 1987; Oberhauser, Alvarez & Latorre, 1988; McManus & Magleby, 1991; McManus, 1991; Cui et al., 1997). Muñoz et al. (1998) recently reported an n_H of 8 from cell attached patches of guinea pig smooth muscle and a K_d of 1 μM $[Ca^{2+}]_i$. One suggested mechanism to account for observed differences between the intact cell and other studies was the loss of regulation by cytoplasmic proteins in the native cell (Muñoz et al., 1998). The high n_H we report for *rbslo1* and the reduction in the *delA* form strongly suggests that the insertion plays a role in the Ca^{2+} sensitivity of the voltage sensor.

In native channels from rat skeletal muscle addition of 10 mM Mg^{2+} to the cytoplasmic surface increased Ca^{2+} affinity and the n_H increased from 2 to 4.5 (Golowasch, Kirkwood & Miller, 1986). Other divalent cations, Co^{2+}, Mn^{2+}, Ni^{2+}, Cd^{2+}, also increased Ca^{2+} affinity and increased n_H when applied to the cytoplasmic surface (Oberhauser et al., 1988). The increased cooperativity was thought to be due to binding of modulatory sites on the protein because surface charge screening effects would affect the apparent Ca^{2+} binding but not change n_H (Oberhauser et al., 1988). Saito et al., (1997) demonstrated that even though an insertion at site A shifted activation by 20–30 mV, addition of Mg^{2+} shifted $V_{1/2}$ an additional 60 mV. This implies that the Mg^{2+} and the insertion act at different sites, but it is possible that their insertion had lower efficacy than Mg^{2+} at a single modulatory site. Thus one possibility is that the differences in *rbslo1* occur at the Mg^{2+} regulatory site.

In summary, the splice variant, *rbslo1* is highly homologous with other cloned *slo* channels yet exhibits profound differences in activation characteristics when compared to clones expressed in other experimental systems such as *Xenopus* oocytes (Butler et al., 1993; McCobb et al., 1995; Cui et al., 1997; Saito et al., 1997; Xie & McCobb, 1998). Ca^{2+} affinity and n_H for *rbslo1* in excised patch are very similar to values reported from cell attached recordings of native channels in guinea pig

smooth muscle (Muñoz et al., 1998). The channel gating exhibited by *delA* is similar to that of other cloned MaxiK channels recorded from a variety of expression systems and recording configurations. The differences between *rbslo1* and other cloned channels appear to be localized at insertion site A with both the insertion sequence and amino acid substitutions near site A being important. The insertion plays a critical role in channel function by allowing the channel to activate at very low $[Ca^{2+}]_i$ while the steep activation curve increases the channel responsiveness to small membrane depolarization. Identification of *rbslo1* which has a much higher Ca^{2+} sensitivity and is more active at negative membrane voltages raises the possibility that splice variants of Ca^{2+}-activated K^+ channels expressed in kidney do play a role in renal K^+ transport.

This work was supported by National Institutes of Health grant DK-32753.

References

Barrett, J.N., Magleby, K.L., Pallotta, B.S. 1982. Properties of single calcium-activated potassium channels in cultured rat muscle. *J. Physiol.* **331:**211–230

Brooks, S.P.J., Storey, K.B. 1992. Bound and determined: a computer program for making buffers of defined ion concentrations. *Anal. Biochem.* **201:**119–126

Butler, A., Tsunoda, S., McCobb, D.P., Wei, A., Salkoff, L. 1993. *mslo*, a complex mouse gene encoding "Maxi" calcium-activated potassium channels. *Science* **261:**221–224

Colquhoun, D., Sakmann, B. 1985. Fast events in single-channel currents activated by acetylcholine and its analogues at the frog muscle end-plate. *J. Physiol.* **369:**501–557

Colquhoun, D., Sigworth, F.J. 1995. Fitting and statistical analysis of single-channel records. *In:* Single-Channel Recording. pp. 483–587. Plenum Press, New York

Cornejo, M., Guggino, S.E., Guggino, W.B. 1987. Modification of Ca^{2+}-activated K^+ channels in cultured medullary thick ascending limb cells by N-bromoacetamide. *J. Membrane Biol.* **99:**147–155

Cox, D.H., Cui, J., Aldrich, R.W. 1997. Allosteric gating of a large conductance Ca-activated K^+ channel. *J. Gen. Physiol.* **110:**257–281

Cui, J., Cox, D.H., Aldrich, R.W. 1997. Intrinsic voltage dependence and Ca^{2+} regulation of *mslo* large conductance Ca-activated K^+ channels. *J. Gen. Physiol.* **109:**647–673

De Lean, A., Munson, P.J., Rodbard, D. 1978. Simultaneous analysis of families of sigmoidal curves: application to bioassay, radioligand assay, and physiological dose-response curves. *Am. J. Physiol.* **234:**E97–E102

Devidas, S., Yue, H., Guggino, W.B. 1998. The second half of the cystic fibrosis transmembrane conductance regulator forms a functional chloride channel. *J. Biol. Chem.* **273:**29373–29380

Golowasch, J., Kirkwood, A., Miller, C. 1986. Allosteric effects of Mg^{2+} on the gating of Ca^{2+}-activated K^+ channels from mammalian skeletal muscle. *J. Exp. Biol.* **124:**5–13

Guggino, S.E., Guggino, W.B., Green, N., Sacktor, B. 1987. Ca^{2+}-activated K^+ channels in cultured medullary thick ascending limb cells. *Am. J. Physiol.* **252:**C121–C127

Guggino, S.E., Suarez-Isla, B.A., Guggino, W.B., Sacktor, B. 1985. Forskolin and antidiuretic hormone stimulate a Ca^{2+}-activated K^+ channel in cultured kidney cells. *Am. J. Physiol.* **249:**F448–F455

Hamill, O.P., Marty, A., Neher, E., Sakmann, B., Sigworth, F.J. 1981. Improved patch-clamp techniques for high-resolution current recording from cells and cell-free membrane patches. *Pfluegers Arch.* **391:**85–100

Hille, B. 1992 Ionic Channels of Excitable Membranes. 607 pp. Sinauer Associates, Sunderland, MA

Knaus, H.G., Folander, K., Garcia-Calvo, M., Garcia, M.L., Kaczorowski, G.J., Smith, M., Swanson, R. 1994. Primary sequence and immunological characterization of beta-subunit of high conductance $Ca^{(2+)}$-activated K^+ channel from smooth muscle. *J. Biol. Chem.* **269:**17274–17278

Lagrutta, A., Shen, K.-Z., North, R.A., Adelman, J.P. 1994. Functional differences among alternatively spliced variants of *slowpoke*, a *Drosophila* calcium-activated potassium channel. *J. Biol. Chem.* **269:**20347–20351

Ling, B.N., Hinton, C.F., Eaton, D.C. 1991. Potassium permeable channels in primary cultures of rabbit cortical collecting tubule. *Kidney Int.* **40:**441–452

McCobb, D.P., Fowler, N.L., Featherstone, T., Lingle, C.J., Saito, M., Krause, J.E., Salkoff, L. 1995. A human calcium-activated potassium channel gene expressed in vascular smooth muscle. *Am. J. Physiol.* **269:**H767–H777

McManus, O.B. 1991. Calcium-activated potassium channels: regulation by calcium. *J. Bioenerg. Biomembr.* **23:**537–560

McManus, O.B., Helms, L.M., Pallanck, L., Ganetzky, B., Swanson, R., Leonard, R.J. 1995. Functional role of the beta subunit of high conductance calcium-activated potassium channels. *Neuron* **14:**645–650

McManus, O.B., Magleby, K.L. 1991. Accounting for the $Ca^{(2+)}$-dependent kinetics of single large-conductance $Ca^{(2+)}$-activated K^+ channels in rat skeletal muscles. *J. Physiol.* **443:**739–777

Meera, P., Wallner, M., Song, M., Toro, L. 1997. Large conductance voltage- and calcium-dependent K^+ channel, a distinct member of voltage-dependent ion channels with seven N-terminal transmembrane segments (S0–S6), an extracellular N terminus, and in intracellular (S9–S10) C terminus. *Proc. Natl. Acad. Sci. USA* **94:**14066–14071

Merot, J., Bidet, M., Maout, S.L., Tauc, M., Pojeol, P. 1989. Two types of K^+ channels in the apical membrane of rabbit proximal tubule in primary culture. *Biochim. Biophys. Acta* **978:**134–144

Morita, T., Hanaoka, K., Morales, M.M., Montrose-Rafizadeh, C., Guggino, W.B. 1997. Cloning and characterization of maxi K^+ channel β-subunit in rabbit kidney. *Am. J. Physiol.* **273:**F615–F624

Muñoz, A., Garcia, L., Guerrero-Hernandez, A. 1988. *In situ* characterization of the Ca^{2+} sensitivity of large conductance Ca^{2+}-activated K^+ channels: implications for their use as near-membrane Ca^{2+} indicators in smooth muscle cells. *Biophys. J.* **75:**1774–1782

Oberhauser, A., Alvarez, O., Latorre, R. 1988. Activation by divalent cations of a Ca^{2+}-activated K^+ channel from skeletal muscle membrane. *J. Gen. Physiol.* **92:**67–86

Okada, Y., Hazama, A., Oiki, S. 1988. [Ca-selective electrode]. *Sentai no Kagaku* **39:**352–354 [Japanese]

Rothberg, B.S., Magleby, K.L. 1999. Voltage-dependent steps in the gating of single BK channels. *Biophys. J.* **76:***A*333 (*Abstr.*)

Saito, M., Nelson, C., Salkoff, L., Lingle, C.J. 1997. A cysteine-rich domain defined by a novel exon in a *slo* variant in rat adrenal chromaffin cells and PC12 cells. *J. Biol. Chem.* **272:**11710–11717

Schreiber, M., Salkoff, L. 1997. A novel calcium-sensing domain in the BK channel. *Biophys. J.* **73:**1355–1363

Shen, K.Z., Lagrutta, A., Davies, N.W., Standen, N.B., Aldeman, J.P., North, R.A. 1994. Tetraethylammonium block of slowpoke cal-

cium-activated potassium channels expressed in *Xenopus* oocytes: evidence for tetrameric channel formation. *Pfluegers Arch.* **426:**440–445

Tseng-Crank, J., Foster, C.D., Krause, J.D., Mertz, R., Godinot, N., DiChiara, T.J., Reinhart, P.H. 1994. Cloning, expression, and distribution of functionally distinct Ca^{2+}-activated K^+ channel isoforms from human brain. *Neuron* **13:**1315–1330

Wallner, M., Meera, P., Toro, L. 1996. Determinant for β-subunit regulation in high-conductance voltage-activated and Ca^{2+}-sensitive K^+ channels: an additional transmembrane region at the N terminus. *Proc. Natl. Acad. Sci. USA* **96:**14922–14927

Wright, J.M., Kline, P.A., Nowak, L.M. 1991. Multiple effects of tetraethylammonium on N-methyl-D-aspartate receptor-channels in mouse brain neurons in cell culture. *J. Physiol.* **439:**579–604

Xie, J., McCobb, D.P. 1998. Control of alternative splicing of potassium channels by stress hormones. *Science* **280:**443–446